

# Trajectory Optimization Procedures for Rotorcraft Vehicles Including Pilot Models, with Applications to ADS-33 MTEs, Cat-A and Engine Off Landings\*

Carlo L. Bottasso<sup>†</sup>, Giorgio Maisano<sup>‡</sup>, Francesco Scorcelletti<sup>§</sup>  
Politecnico di Milano – AgustaWestland  
Milano, Italy

## Abstract

*The present paper focuses on trajectory optimization problems for rotorcraft vehicles, accounting for the presence of pilot-in-the-loop effects. In previous papers we have developed numerical procedures for trajectory optimization which can cater to a wide range of vehicle models of varying complexity. The trajectory optimal control problem is solved through a direct approach by means of transcription or multiple shooting methods, depending on the model complexity and problem characteristics. Specific focus of the present work is the inclusion of pilot models in the optimization process, in order to improve the fidelity of the solution by considering the entire coupled human-vehicle system. In particular we are interested in investigating a series of maneuvers quantifying the performance loss, due to human limitations, of the pilot-rotorcraft system with respect to the sole vehicle case. A number of examples are considered in order to analyze this issue.*

## INTRODUCTION

The ability to simulate maneuvers of rotorcraft vehicles flying at the boundaries of their operating envelope is a valuable asset for performance analysis, handling qualities research, design and certification, pilot training, and support to the flight test activity. In general the maneuver of interest can be fully described in terms of quantities which should be minimized or maximized, subject to a variety of equality and inequality constraints [10, 8, 9, 11, 13]. Hence, one can usually give a precise definition of a maneuver by formulating an equivalent optimal control problem. The formulation of such a problem necessitates of a model of the vehicle system with its inputs, states and outputs, of a cost function and of a list of all constraints.

Clearly, the fidelity of the predictions made using this approach crucially hinges on the fidelity of the vehicle model. On the one hand, fidelity improvements may be obtained by considering for example more sophisticated aerodynamics and/or a more detailed structural description of the vehicle; on the other hand, one might clearly consider the inclusion of a model of the pilot. In fact, in the absence of a pilot model, the solution

of a trajectory optimization problem amounts to finding the limit performance trajectory flyable by a “perfect” pilot. In reality, the pilot is a complex system which can be modeled so as to account for sensory perceptions, learned behavior and biomechanical properties. Therefore, it is reasonable to assume that a maneuver optimized considering just a flight mechanics model of the vehicle will in general tend to overestimate the vehicle performance, as this has been computed without accounting for the limitations of various nature of a real pilot. To verify whether this is indeed the case, the present work tries to quantify this hypothesized performance loss due to the inclusion of a pilot model in the trajectory optimization process. To our knowledge, this paper represent the first time that trajectory optimization procedures for rotorcraft vehicles are proposed and formulated accounting for pilot-in-the-loop effects.

A human pilot model should account for various effects:

- **Sensorial perception:** the sensorial system of the pilot provides for a perception of movements, body position, accelerations, vibrations, etc., which enable the pilot to build a representation of the current situation.
- **Control behavior:** the pilot, based on the input provided by the sensorial information, evaluates the situation and, on the basis of a desired goal,

\*Presented at the American Helicopter Society 65th Annual Forum and Technology Display, May 27–29, 2009, Gaylord Texan Resort and Convention Center, Grapevine, TX, USA.

<sup>†</sup>Associate Professor, e-mail: [carlo.bottasso@polimi.it](mailto:carlo.bottasso@polimi.it).

<sup>‡</sup>Ph.D. candidate.

<sup>§</sup>Ph.D. candidate, AgustaWestland flight mechanics engineer.

elaborates a control law based on experience and training.

- **Command actuation:** the neuromusculoskeletal system of the pilot acts like an actuator that takes as input the control law and translates it into movements of the vehicle controls (collective, cyclics, pedal).

In the literature, there is a wide range of pilot models which have been formulated for different applications. As suggested in Ref. [20], pilot models can be subdivided in the following categories:

- **Crossover Model:** a basic model for single-axis tracking tasks, which is useful for tuning more complete models. In the region of the open-loop crossover frequency, the product of the pilot transfer function and that of the vehicle is approximated as an integrator with time delay [25].
- **Isomorphic Models:** all models which try to explicitly approximate the dynamics of the human sensory and control systems. The *Structural Model* offers a simplified structural representation of the pilot dynamics in compensatory systems [29, 19]. Particular emphasis is given to sensorial feedback, which typically includes proprioceptive and vestibular feedbacks, while the neuromuscular components of the model is approximated with a second order filter. The *Biophysical Models* give more emphasis to the dynamics of the pilot neuromuscular system [27]. Finally, *Biodynamic Models* are based on multi-body dynamics approaches [21], and are used for investigating the effects of an accelerating/vibrating environment on the pilot control capabilities.
- **Algorithmic Models:** models whose principal focus is the control behavior of the pilot, but which may include some isomorphism achieving a good degree of completeness. A typical example of this category is the *Optimal Control Model*, which considers the human pilot as an optimal controller [16], and where the sensorial component is taken into account by using a Kalman filter.
- **Behavioral Models:** models which consider the human pilot as a black box with nonlinear behavior. There are two principal approaches in this category: *Fuzzy-Logic Models*, which are based on fuzzy-set theory describing cause-and-effect relationships [24, 29], and *Neural Network Models*, which rely upon the capabilities of neural networks of accurately describing nonlinear input-output relationships, mapping pilot cues into control tasks [22].

Clearly, the most appropriate choice of a pilot model is strictly related to the particular application considered. In the framework of trajectory optimization, we need to account for all three aspects listed above, namely sensorial perception, control behavior, and command actuation. Furthermore, it would be preferable to work with a model formulated in state space form, so as to ease its integration in the overall maneuver optimal control problem.

The sensorial perception can be modeled by formulating appropriate observers, for example using Kalman filtering [16]. As a first step towards the goals set forth in this study, we have neglected this aspect of the problem in the present paper, although we plan on considering it in the continuation of this activity. In fact, although the inclusion of an observer in the maneuver optimal control problem formulation does not pose conceptual difficulties, we have postponed the modeling of this component of the pilot system because of the difficulty in finding data for the tuning of the filters.

The second aspect of the modeling, i.e. the control behavior, is in part already included in the formulation of a maneuver optimal control problem. In fact, the pilot elaborates a control law based on desired goals and constraints, which are in fact the very cost function and constraints which enter into the definition of the optimal control problem. However, some aspects of the control behavior are more subtle and difficult to model, such as for example the skills and experience of the pilot. Such effects are hard to model in precise mathematical terms, but we speculate here that they might be rendered through appropriate modifications of the cost function. For example, piloting skills modeling might account for degraded piloting behavior for maneuvers which require increased coordination and activity among the controls (increased workload) [14]. Such effects are easily included in the proposed maneuver optimal control approach, since the coding requires trivial modifications to the cost function routines. Nonetheless, specific experimental data are lacking, so that even in this case we have not considered these aspects in the present work, while waiting to perform experiments with pilots in a simulator to gather the observations necessary for the tuning of such models. Therefore, in this paper the control behavior is translated in the choice of a cost function that includes a problem-dependent goal quantity (e.g. altitude loss, time, etc.), and a control term which penalizes excessive control activity and/or excessive control rates; specific details on the choice of the cost functions are given below in the section of the paper devoted to the applications. Such modeling, although rather simple, probably captures a significant, and possibly the most significant, part of the pilot behavior.

The third aspect of the problem, the command actuation, can be modeled in a variety of ways. The more

sophisticated approach is based on first-principle modeling of the musculoskeletal system using multibody dynamics, and typically includes rigid bodies with their inertial parameters, joints, muscles with their mechanical and physiological properties, interactional forces with the environment, and other components as required for the accurate representation of the real bio-system. Such level of detail is probably not necessary for capturing the effects of the limitations of the bio-system on the vehicle flight mechanics performance. Hence, a simpler approach is used here, where the effects of the musculoskeletal system are rendered in a global equivalent sense through the use of simple delay and filter models, as detailed below.

There are two principal approaches to the solution of trajectory optimization problem: indirect [15, 28] and direct methods [5, 6, 7, 10, 13]. Following our previous work [11], we prefer the direct approach even for the present paper. In fact, in the case of the indirect methods one has first to derive the optimal control governing equations by using the calculus of variation, and then numerically solve the arising two-point boundary value problem. The manipulation of the vehicle equations of motion for deriving the optimal control governing equations makes it very hard or inefficient, if not altogether impossible, to use black-box flight simulators, where more often than not one does not have access to the source code. In the case of coupled vehicle-pilot models, the equations tend to become even more involved, so that here again the use of a direct approach allows for a simpler implementation. In fact, the direct approach does not require any manipulation of the equations, as one first discretizes the problem by time stepping (using either a transcription or a shooting method [11]) and then solves the resulting Non-Linear Programming (NLP) problem by a standard solver, such as SQP (Sequential Quadratic Programming).

The paper is organized according to the following plan. At first, we describe the pilot model considered in this work and we present the equations of the coupled pilot-rotorcraft system. Secondly, we formulate in general terms the trajectory optimization problem. A discussion about the possible numerical solution strategies to solve this problem are given next; namely, we first describe the direct transcription approach and then we review the direct multiple shooting method. Finally, we investigate a number of maneuvering rotorcraft problems, and we assess the pilot-in-the-loop effects on the computed limit performance of the vehicle.

## COUPLED PILOT-ROTORCRAFT MODEL

As argued in the introduction, enriching the flight mechanical rotorcraft model by adding a pilot model is a way to improve the performance predictions made us-

ing trajectory optimization. The main task of a pilot is to govern the rotorcraft by deciding a suitable control law in relation with the maneuver goals, based on the current perception of the situation as provided by his/her sensory system. The optimal control model proposed in Ref. [23] and revisited in Ref. [16] is a possible way of translating these effects. In the present work we adopt a similar approach, reformulating it in the context of trajectory optimization. This way, the decision level control behavior of the pilot can be considered as embedded in the objective function of the maneuver optimal control problem.

The two remaining aspects of human pilot limitations are due to sensorial perceptions and command actuation. As a first step towards the more ambitious goal of a complete pilot modeling system, we consider here a simple actuator pilot model (Fig. 1), in order to assess its impact on the vehicle performance predictions, as well as on the computational cost and robustness of the numerical procedures.

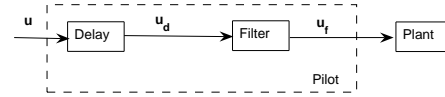


Figure 1: Pilot model: pure delay and second-order filter.

The rotorcraft equations of motion can be expressed as

$$\mathbf{f}(\dot{\mathbf{x}}, \mathbf{x}, \mathbf{u}, t) = 0, \quad (1)$$

where  $\mathbf{x}$  are the flight mechanics states, and  $\mathbf{u}$  the vehicle control inputs (collective, longitudinal and lateral cyclics, and pedal).

The pilot actuator system is modeled using a pure time delay [16], operating in series with a second order filter for the neuromuscular element [29] for each control input. The pure time delay is approximated by a second-order Padè transfer function, which provides excellent accuracy over the frequency range of the pilot (0.1 – 10 rad/sec) [16]; for the single channel we have:

$$Y_d(s) = \frac{1 - \frac{1}{2}(\tau s) + \frac{1}{8}(\tau s)^2}{1 + \frac{1}{2}(\tau s) + \frac{1}{8}(\tau s)^2}. \quad (2)$$

The second-order filter [29] is written as

$$Y_f(s) = \frac{\omega_{NM}^2 s}{s^2 + 2\zeta_{NM}\omega_{NM}s + \omega_{NM}^2}. \quad (3)$$

The series of delay and filter on each control channel can be written in linear state space form as

$$\dot{\mathbf{x}}_p = \mathbf{A}\mathbf{x}_p + \mathbf{B}\mathbf{u}, \quad (4a)$$

$$\mathbf{u}_f = \mathbf{C}\mathbf{x}_p + \mathbf{D}\mathbf{u}, \quad (4b)$$

where  $x_p$  is the neuromuscular state, of length  $4n_u$ , where  $n_u$  is the number of control inputs to be filtered. The elements of matrices  $\mathbf{A}$ ,  $\mathbf{B}$ ,  $\mathbf{C}$  and  $\mathbf{D}$  depend on the delay and filter parameters, and in particular on the time constant  $\tau$  of the pure delay and on the damping factor  $\zeta_{\text{NM}}$  and undamped natural frequency  $\omega_{\text{NM}}$  of the open-loop neuromuscular system. Referring to Fig. 1, it should be noted that the inputs of the pure time delay module are the “desired” command pilot inputs  $\mathbf{u}$ , while the inputs of the neuromuscular module are the delayed command inputs  $\mathbf{u}_d$ . Finally, the delayed and filtered inputs  $\mathbf{u}_f$  actuate the rotorcraft vehicle model.

Collecting together Eqs. (1) and (4), we can write the governing equations of the coupled pilot-rotorcraft model as

$$\dot{x}_p = \mathbf{A}x_p + \mathbf{B}\mathbf{u}, \quad (5a)$$

$$\mathbf{u}_f = \mathbf{C}x_p + \mathbf{D}\mathbf{u}, \quad (5b)$$

$$\mathbf{f}(\dot{x}, x, \mathbf{u}_f, t) = 0. \quad (5c)$$

Formally, by collecting all states in a unique state vector  $\mathbf{x}_{\text{pr}}^T = (\mathbf{x}^T, \mathbf{x}_p^T)^T$ , by collecting all dynamic equations (5) into a single function  $\mathbf{f}_{\text{pr}}$  and eliminating all algebraic equations, we can write the governing equations of the coupled pilot-rotorcraft system in the following compact form:

$$\mathbf{f}_{\text{pr}}(\dot{\mathbf{x}}_{\text{pr}}, \mathbf{x}_{\text{pr}}, \mathbf{u}, t) = 0. \quad (6)$$

When optimizing a maneuver considering only the stand-alone vehicle model, one uses Eqs. (1); on the other hand, when the pilot is included in the optimization the augmented system (6) is used. Formally, the two are identical, so that no changes are necessary to the trajectory optimization software for dealing with the coupled pilot-vehicle model.

## FORMULATION OF MANEUVERS AS OPTIMAL CONTROL PROBLEMS

A maneuver can be defined as a dynamic transition between two steady state configurations [17], although in the present context it is useful to give a looser interpretation of the term by considering also the case of terminal conditions which are not trimmed. Clearly, given a starting and arrival trim, there is an infinite number of ways to transition between the two. A possible way to remove this arbitrariness is to formulate a maneuver as a constrained optimal control problem [8, 9, 10, 13].

The maneuver optimal control problem requires the minimization or maximization of a cost or merit function (e.g. time, altitude loss, control activity, fuel consumption, etc.), which in general can be expressed in terms of the vehicle states or outputs and of the control inputs. Furthermore, the optimization problem is constrained by a number of conditions that should be met by the solution:

- First, the so-called compatibility conditions must be fulfilled at each time instant of the maneuver; in other words, it is required that the computed solution satisfies the equations of motion of a suitable flight mechanics model.
- Second, the solution should remain within the flight envelope and operational limits of the vehicle.
- Finally, most maneuvers of practical interest (Category-A, ADS-33, flare at the exit of an autorotation, etc.) are typically characterized by other equality and inequality constraints which need to be met in order to satisfy given performance and procedural requirements and that, collectively, contribute to giving a precise definition of the maneuver of interest.

The maneuver optimal control problem can be formally expressed as:

$$\min_{\mathbf{x}, \mathbf{y}, \mathbf{u}, T} J = \phi(\mathbf{y}, t)|_0^T + \int_0^T L(\mathbf{y}, \mathbf{u}, \dot{\mathbf{u}}, t) dt, \quad (7a)$$

$$\text{s.t.: } \mathbf{f}(\dot{x}, x, \mathbf{u}) = 0, \quad (7b)$$

$$\mathbf{y} = \mathbf{h}(x), \quad (7c)$$

$$\mathbf{g}(\mathbf{y}, \mathbf{u}, t) \in [\mathbf{g}^{\min}, \mathbf{g}^{\max}]. \quad (7d)$$

Solving the problem consists in finding the control function  $\mathbf{u}(t)$ , and hence through (7b) and (7c) the associated functions  $x(t)$  and  $y(t)$ , which minimize the cost  $J$  given by Eq. (7a). In general, the cost includes a boundary quantity which accounts for values of the outputs at the initial and/or final instants, as well as an integral cost term. The problem is defined on the interval  $\Omega = [0, T]$ ,  $t \in \Omega$ , where the final time  $T$  is typically unknown and must be determined as part of the solution to the problem.

The model governing equations appear among the problem constraint conditions, and are expressed by Eqs. (7b) and (7c), where  $x$  are the states,  $\mathbf{u}$  the inputs and  $y$  the outputs. As shown in the previous section, the model governing equations (7b) can be represented by Eqs. (1) when considering the stand-alone vehicle model, or by Eqs. (6) for the coupled pilot-vehicle case.

All maneuver-defining and/or envelope-protection constraints are expressed as generic algebraic nonlinear constraints by Eqs. (7d). These may include as special cases boundary (initial ( $t = 0$ ) and/or terminal ( $t = T$ )) conditions, constraints at unknown internal time events ( $t = T_i$ ), generic constraints defined over the whole maneuver duration ( $t \in [0, T]$ ), which clearly may also include, as it is often the case in practical applications, simple bounds on the inputs and states/outputs.

## DIRECT SOLUTION OF MANEUVER OPTIMAL CONTROL PROBLEMS

As discussed in Ref. [11], the direct approach is often the preferable way to solve the optimal control problem (7), for a series of practical advantages with respect to the classical indirect method. According to the direct approach, the optimal control problem is first discretized and subsequently optimized. This procedure yields a discrete parameter optimization or NLP problem [18], which can be written as

$$\min_z K(\mathbf{z}), \quad (8a)$$

$$\text{s.t. } \mathbf{a}(\mathbf{z}) = \mathbf{0}, \quad (8b)$$

$$\mathbf{b}(\mathbf{z}) \in [\mathbf{b}^{\min}, \mathbf{b}^{\max}], \quad (8c)$$

where  $\mathbf{z}$  is a vector of algebraic unknowns, and  $K$  is a scalar objective function which represents an approximation of the cost  $J$  of Eq. (7a). The equality constraints (8b) are generated by the discretization of the equations of motion (7b,7c), while the inequality constraints (8c) by all other maneuver-defining constraints (7d). Notice that the problem defined by (8) is characterized by unknown algebraic parameters  $\mathbf{z}$ , while the optimal control problem (7) by functional unknowns.

The specific form of the vector of algebraic unknowns and of the constraints in problem (8) depends on the method used for performing the discretization. Our software program TOP (Trajectory Optimization Program) [11] implements both the direct transcription and the direct multiple shooting methods, which are briefly reviewed next.

### Direct Transcription

This method is very effective and robust, but it is typically applicable only to models which have low-moderate complexity [13], i.e. which do not have solution time scales which are too fast with respect to the overall maneuver duration, and/or do not possess too large a number of states.

The time interval  $\Omega$  is partitioned as  $0 = t_0 < t_1 < \dots < t_N = T$ , where the generic time element is  $\Omega^n = [t_n, t_{n+1}]$ ,  $n = (0, N-1)$ , of time step size  $h^n = t_{n+1} - t_n$ . On each time element  $\Omega^n$ , the governing equations (7b) are discretized using a suitable numerical method. The resulting discrete equations are expressed as

$$\mathbf{f}_h(\mathbf{x}_{n+1}, \mathbf{x}_n, \mathbf{u}^n, h^n) = \mathbf{0}, \quad n = (0, N-1), \quad (9)$$

where  $\mathbf{f}_h$  is an algorithmic approximation of function  $\mathbf{f}$  of Eq. (7b),  $\mathbf{x}_n, \mathbf{x}_{n+1}$  are the values of the state vector at  $t_n$  and  $t_{n+1}$ , respectively, while  $\mathbf{u}^n$  represents the value of the control vector within the step. In general there might be additional internal stages for both the state

and the control variables, depending on the numerical method [11].

The NLP problem (8) is defined as follows. First, the NLP vector of parameters is chosen as:

$$\mathbf{z} = (\mathbf{x}_{n=(0,N)}, \mathbf{u}^{n=(0,N-1)}, T)^T, \quad (10)$$

i.e. it is defined by the discrete states and control values on the computational grid, and the final time. Notice that, if one needs a very large number of time steps to accurately resolve the solution, the size of  $\mathbf{z}$  will be large, up to the point of making this approach unsuitable in terms of computational burden.

Next, the cost  $J$  of Eq. (7a) is discretized in terms of  $\mathbf{z}$  as given by (10), obtaining the discrete cost  $K$  of Eq. (8a). Then, the discretized ODEs within each step, Eqs. (9), become the set of NLP equality constraints appearing in Eq. (8b). Finally, all other problem constraints and bounds, Eqs. (7d), are expressed in terms of the NLP variables  $\mathbf{z}$  and become the NLP inequality constraints of Eq. (8b).

### Direct Multiple Shooting

This method is typically used in applications of moderate/high complexity, i.e. with solution time scales which are fast with respect to the maneuver duration, and/or a moderate/large number of degrees of freedom [13].

The time domain  $\Omega$  is partitioned as  $0 = t_0 < t_1 < \dots < t_M = T$  with  $\Omega^m = [t_m, t_{m+1}]$ ,  $m = (0, M-1)$ , where each  $\Omega^m$  is a shooting segment. In each shooting segment  $\Omega^m$ , the controls are discretized as  $\mathbf{u}^m(t) = \sum_{i=1}^{N_c^m} s_i(t) \mathbf{u}_i^m$ , where  $s_i(t)$  are basis functions, in particular cubic splines in the present implementation, and  $\mathbf{u}_i^m$  are  $N_c^m$  unknown discrete control values. The control approximations are confined on each shooting segment, which has the effect of decreasing the computational cost of finite differencing by increasing the problem sparsity. Constraints are enforced at the shooting segment boundaries to guarantee the continuity of the controls up to  $C^1$ .

In the case of direct multiple shooting, the NLP problem (8) is defined as follows. First, the NLP unknown parameters are chosen as:

$$\mathbf{z} = (\mathbf{x}_{m=(0,M)}, \mathbf{u}_{i=(1,N_c^m)}^{m=(0,M-1)}, T)^T, \quad (11)$$

i.e. they represent the discrete values of the states at the interfaces between shooting segments, the discrete values of the controls within each segment, and the final time.

Next, the governing ODEs (7b) are marched in time within each shooting segment  $\Omega^m$ , starting from the initial conditions provided by the values of the states  $\mathbf{x}_m$  at the left boundary of the segment. The effect of the forward integration is to generate a discrete time history of states within  $\Omega^m$ , which we label  $\mathbf{x}_i^m$ ,  $i = (1, N^m)$ ,

where  $N^m$  is the number of steps taken in that segment. The last value of this sequence is named  $\tilde{\mathbf{x}}_{m+1} = \mathbf{x}_{N^m}^m$ , and represents the new estimate of the state variables at the right boundary of the shooting segment. Segments are then glued together by imposing the following equality constraints

$$\mathbf{x}_m - \tilde{\mathbf{x}}_m = 0, \quad m = (2, M). \quad (12)$$

Multiple shooting segments are used for stabilizing the forward integration of the vehicle equations of motion [4]. This is particularly important when analyzing unstable systems, which is often the case when considering rotorcraft vehicles.

Notice that the size of the unknown parameter vector  $\mathbf{z}$  is uncorrelated to the time step size using for marching the equations of motion within shooting arcs; hence, one may use very fine temporal discretizations without impacting the overall problem size, which in fact enables the solution of problems with a higher degree of complexity than in the direct transcription case [13].

In the direct multiple shooting case, the cost  $J$  of Eq. (7a) is discretized in terms of  $\mathbf{z}$  as given by (11) and evaluated using the segment time histories  $\mathbf{x}_i^m$ ; this yields the discrete cost  $K$  of Eq. (8a). Next, the gluing conditions (12) are used to express the set of NLP equality constraints appearing in Eq. (8b). All other problem constraints and bounds, Eqs. (7d), are expressed in terms of the NLP variables  $\mathbf{z}$  and become the NLP inequality constraints of Eq. (8b).

## APPLICATIONS AND RESULTS

In this section we consider the solution of several maneuver optimal control problems of practical interest.

Initially, we analyze the ADS-33 Lateral Reposition Mission Task Element (MTE) [2] for handling qualities assessment, as well as a Category-A rejected take-off [1]. Goal of these two examples is a first preliminary assessment of the effects of the inclusion of the simplified pilot model described earlier on in this work with respect to the computed limit performance.

Next, we consider the Pirouette and Slalom MTEs and an engine-off landing condition. Due to time constraints, these examples have so far been analyzed only for the stand-alone vehicle model, without pilot-in-the-loop effects. The investigation of the presumed performance degradation using the coupled pilot-rotorcraft model will be presented in a forthcoming publication.

The helicopter model, implemented using the FLIGHTLAB code [3], represents a generic medium-size multi-engine four-bladed utility vehicle in the 9 ton class. It is based on three-dimensional rigid body dynamics, where rotor forces and moments are computed by combining actuator disk and blade element theory, considering a uniform inflow [26]; the model also in-

cludes a power balance equation, which relates the rotor speed rate to the power available and to the main and tail rotor torques. The rotor attitude is evaluated by means of quasi-steady flapping dynamics with a linear aerodynamic damping correction. Look-up tables are used for the quasi-steady aerodynamic coefficients of the vehicle lifting surfaces, and simple corrections for compressibility effects and for the downwash angle at the tail due to the main rotor are included in the model.

### Lateral Reposition MTE

The ADS-33E-PRF specification [2] for military rotorcraft defines a series of MTEs which provide a basis for an overall assessment of the vehicle ability to perform certain critical tasks, and result in an assigned level of handling qualities according to the Cooper-Harper rating scale. Each MTE is related to a specific maneuver that shall be accomplished considering specific constraints, as described in Ref. [2]. In fact, it is possible to formulate each MTE as a constrained optimal control problem [12]. Hence, with a software implementation of the procedures discussed in this work, it is possible to readily compile a library of MTEs of interest in order to predict the handling qualities characteristics of a specific rotorcraft and work in parallel with the flight test trials.

We analyze here the Lateral Reposition MTE with a multiple shooting approach, considering both the stand-alone vehicle model and the coupled pilot-rotorcraft system.

According to the Lateral Reposition MTE [2], the helicopter, initially in hover, is supposed to translate laterally for 400 ft and then recover the initial hover configuration. The maneuver must be flown in ground effect since the initial and final positions are characterized by an altitude of 35 ft (the rotor diameter is 30 ft); altitude variations must be within  $\pm 10$  ft. Referring to Fig. 2, the maximum allowed displacement in the longitudinal direction is  $\pm 10$  ft, while the maximum heading misalignment is  $\pm 10$  deg with respect to the initial direction. The maneuver must be completed within 18 sec.

One possible formulation of this MTE is to consider the following minimum time cost function (13):

$$J = T + \frac{1}{T} \int_0^T \dot{\mathbf{u}} \cdot \mathbf{W} \dot{\mathbf{u}} dt. \quad (13)$$

The first term enforces the minimum time condition, while  $\mathbf{W} = \text{diag}(\mathbf{w}_i)$  is a diagonal matrix of tunable weighting factors which penalize the control rates.

It is also necessary to constrain the vehicle trajectory so as to express the MTE path requirements described above. With this formulation of the problem the time constraint is not explicitly enforced, but verified a posteriori. In other words, one tunes the weight parameters  $\mathbf{W}$  in the merit function (13), this way controlling the aggressiveness of the maneuver. Then, once

a solution has been computed, one verifies whether the maneuver was rapid enough and effectively completed within the maximum allotted time. Obviously there are limitations in the maneuver aggressiveness related to the vehicle capabilities and its flight envelope constraints. In this case the trajectory constraints are imposed directly through bounds on the position variables and heading angle:

$$|\psi(t)| \leq 10 \text{ deg}, \quad (14a)$$

$$|x(t)| \leq 10 \text{ ft}, \quad (14b)$$

$$|\Delta z(t)| \leq 10 \text{ ft}, \quad (14c)$$

$$0 \leq y(t) \leq 400 \text{ ft}. \quad (14d)$$

It should be noted that the  $y$ -overshooting is avoided with this approach.

We solved this problem initially without considering a pilot model; once the “pilot-off” solution had been evaluated, we used it as the initial guess for the evaluation of the “pilot-on” case. The following values for the pilot actuator model were used [29]:  $\tau = 0.2$  sec,  $\omega_{NM} = 10$  rad/sec,  $\zeta_{NM} = \cos(\pi/4)$ .

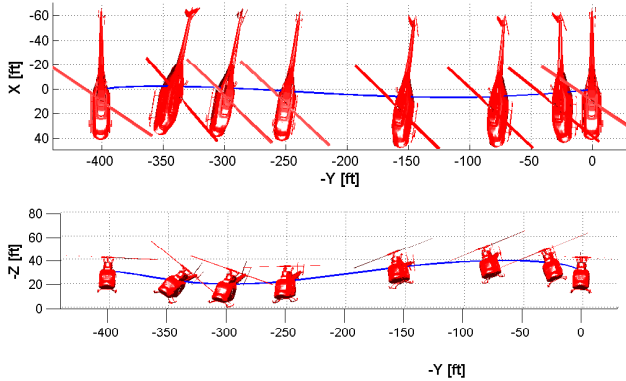


Figure 2: Lateral Reposition MTE: snapshots.

The numerical solution was obtained with the multiple shooting approach, using a sufficiently large number of integration arcs so as to guarantee a good approximation of the MTE trajectory constraints expressed by Eqs. (14). The multiple shooting approach was preferred in this case because the pilot model time scales imply small time steps, which would drive up the grid size and hence the computational cost for the direct transcription method.

Figure 2 shows some snapshots of the helicopter during the maneuver. Figure 3 gives the time histories of the constrained path variables, for both the pilot-off (solid lines) and the pilot-on cases (dash-dotted lines). Figure 4 shows the control time histories.

The pilot-in-the-loop effects do not appear to generate significant differences with respect to the stand-alone vehicle model for both the trajectory and the control inputs. The maneuver duration is in both cases

less than the 18 sec prescribed by the normative, with a slightly longer total time for the pilot-on case. Both trajectory and controls do not appear to have been significantly affected by the neuromuscular lag.

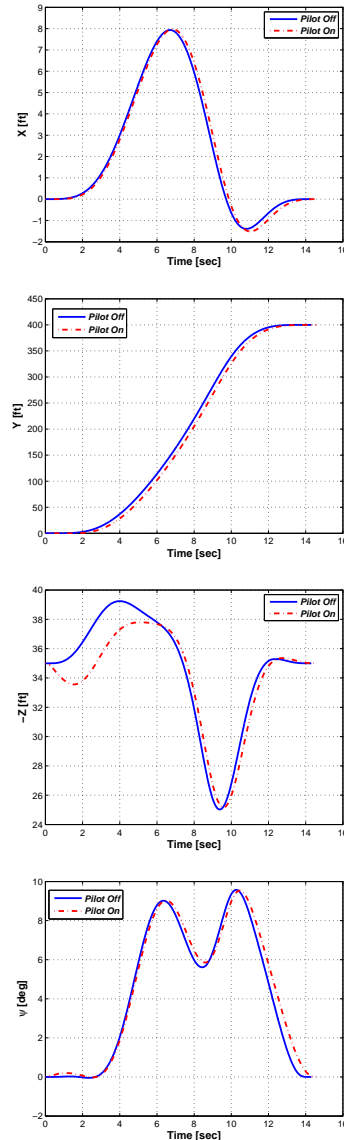


Figure 3: Lateral Reposition MTE: X, Y, Z positions, and heading angle (from top to bottom).

### Category-A Rejected Take-off

The effect of pilot actuation are investigated also for the case of a rejected take-off maneuver under Category A certification requirements [1]. A meaningful simulation policy for such a maneuver consists in the minimization of the altitude loss, according to the cost

$$J = H(T) + \frac{1}{T} \int_0^T \dot{\mathbf{u}} \cdot \mathbf{W} \dot{\mathbf{u}} dt, \quad (15)$$

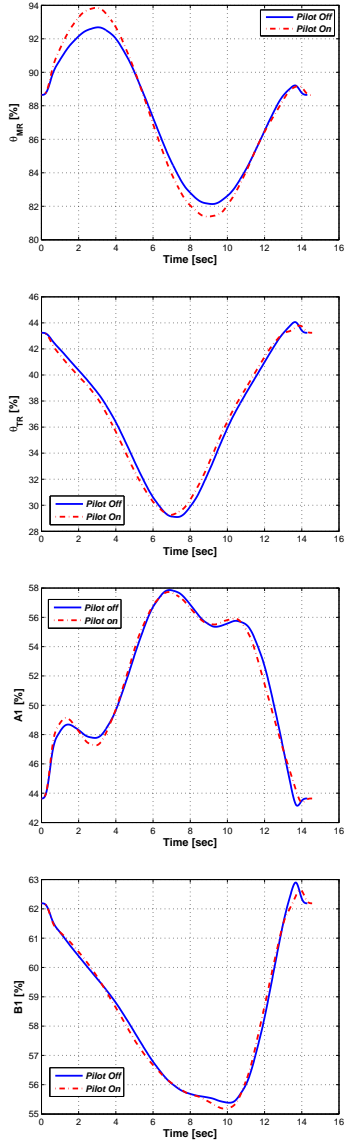


Figure 4: Lateral Reposition MTE: collective, pedal, lateral and longitudinal cyclic (from top to bottom).

The initial condition is a hover. A latency period of 1.2 sec after the engine failure is taken into account, during which the pilot realizes the situation and there is no control activity. The power loss is modeled as

$$P_{av}(t) = P_H + (P_{OEI} - P_H)K^+(t) + P_H K^-(t), \quad (16a)$$

$$K^+(t) = \text{sca}(t - t_0)(1 - e^{-t/\tau^+}), \quad (16b)$$

$$K^-(t) = \text{sca}(t - t_0)e^{-(t-t_0)/\tau^-}, \quad (16c)$$

where  $t_0$  is the instant of engine failure,  $P_H$  is the hover power,  $P_{OEI} = 1750$  HP is the one engine inoperative maximum take-off power available, while  $\tau^+ = 2/9$  sec and  $\tau^- = 1/9$  sec are suitable time constants. The final

conditions are

$$W(T_f) = 0 \text{ m/sec}, \quad (17a)$$

$$p(T_f) = q(T_f) = r(T_f) = 0 \text{ deg/sec}, \quad (17b)$$

$$\Omega(T_f) \geq 90\%. \quad (17c)$$

Because no ground effect was taken into account and we were interested in the altitude loss comparison, the initial altitude was fixed for all simulations to the value  $H(0) = 30$  m.

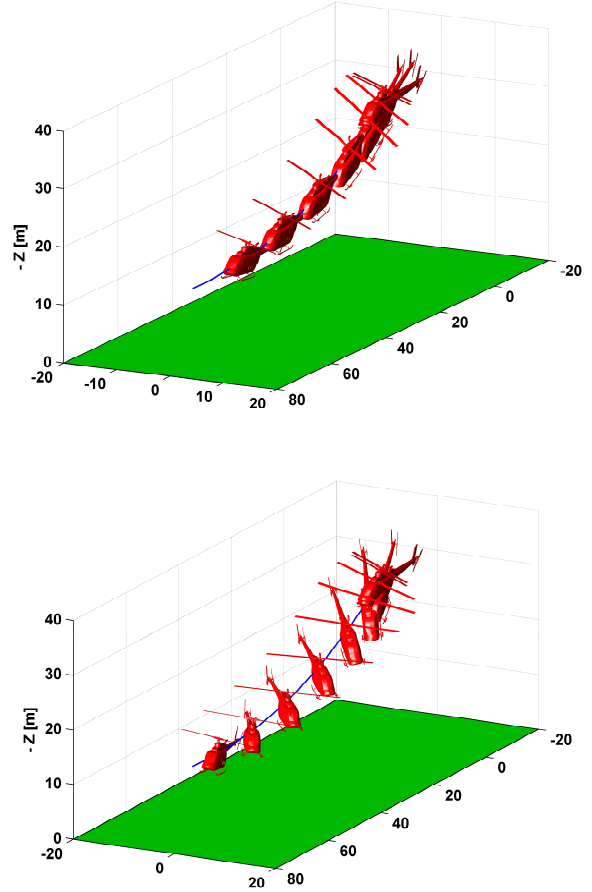


Figure 5: Category A, rejected take-off: optimal two-dimensional (top) and three-dimensional (bottom) trajectories, pilot-off case.

The standard procedure is to fly this emergency maneuver in the longitudinal plane of the helicopter. In fact, simulations of this maneuver are often conducted with a two-dimensional helicopter model. However, using a three-dimensional model, one may observe that the solution converges to a three-dimensional maneuver with significant yaw and roll (see Fig. 5). The three-dimensional (3D) optimal maneuver altitude loss  $\Delta H_{\min}^{3D} = 15.77$  m improves on the two-dimensional (2D) optimal altitude loss  $\Delta H_{\min}^{2D} = 16.72$  m of about one meter (Fig. 6). This gain can be explained by observing

Fig. 7. In the 3D maneuver, both the roll and the yaw angles increase and reach their respective maxima approximately halfway throughout the maneuver. This attitude allows for some reduction in the vertical velocity (Fig. 8), which explains the decreased altitude loss. Clearly, the control activity on the pedal and lateral cyclic is higher for the 3D maneuver than for the 2D one.

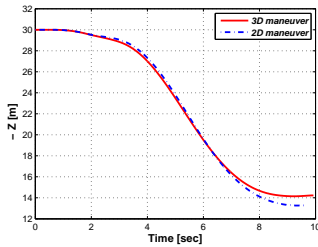


Figure 6: Category A, rejected take-off: altitude loss comparison, pilot-off case.

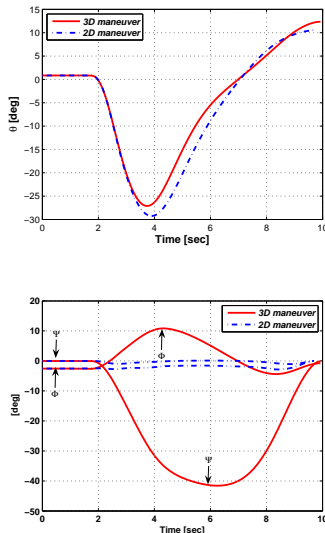


Figure 7: Category A, rejected take-off: helicopter attitude, pilot-off case.

These two simulations were repeated including the pilot model. To simplify convergence, we used a bootstrapping procedure. The first guess was initialized to the solution computed without pilot model. Next, the control time histories of the guess solution were used for evaluating the pilot model dynamic constraints, thus obtaining initial estimates of the pilot state time histories. The stand-alone vehicle solution augmented with the pilot state time histories was then used as initial guess for the pilot-in-the-loop optimization.

For the coupled pilot-vehicle problem, the resulting optimal maneuvers do not change significantly in terms

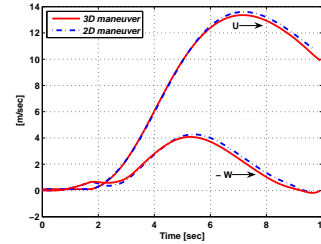


Figure 8: Category A, rejected take-off: inertial velocities, pilot-off case.

of control input profiles with respect to pilot-off simulations, but the altitude loss increases for both the 2D and 3D cases (see Fig. 9). In the 2D maneuver the altitude loss is  $\Delta \hat{h}_{\min}^{2D} = 18.56$  m with a difference of 1.84 m (10.38%) with respect to the pilot-off case, while in the 3D case we obtain  $\Delta \hat{h}_{\min}^{3D} = 17.62$  m with a difference of 1.85 m (11.73%). This is not simply due to the fact that all time histories are delayed. The principal reason appears to be the delay in the pilot first reaction to the engine loss, which gives a higher maximum vertical velocity value, as shown in Fig. 10.

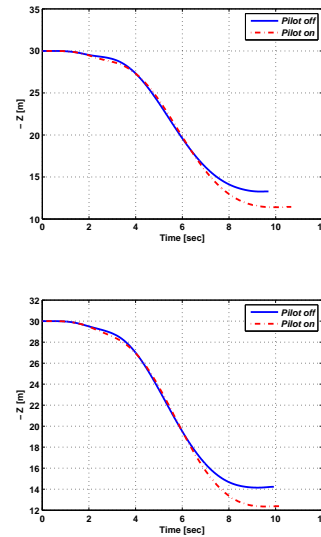


Figure 9: Category A maneuver, rejected take-off: altitude loss comparison (top: 2D; bottom: 3D).

In conclusion, the introduction of a pilot model seems to have a non negligible effect on the performance estimation, which would seem to motivate further refinements in the simplified pilot model considered in this preliminary study. Furthermore, it appears that a 3D maneuver gives better performance (less altitude loss), than the usual 2D one. However, the 3D maneuver is harder to fly since it requires good coordination skills. Moreover, the pronounced sideslipping

might make it difficult for the pilot to hold the visual references.

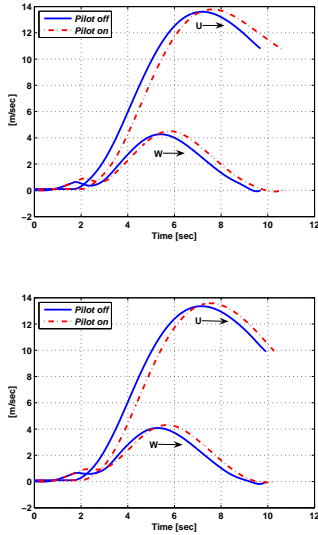


Figure 10: Category A maneuver, rejected take-off: inertial velocities (top: 2D; bottom: 3D).

### Pirouette and Slalom MTEs

We consider the Pirouette and Slalom MTEs, which were simulated by considering just the stand-alone vehicle model. In the future, we will analyze these cases using the coupled pilot-rotorcraft system in order to quantify possible performance degradations.

As described in Ref. [2], for the Pirouette MTE the helicopter should move along a reference circle of radius  $R = 100$  ft, pointing the nose towards the center of the trajectory, starting and arriving in the hover condition. The maneuver must be accomplished while satisfying constraints on the radial displacement, which must be less than  $\Delta R \pm 10$  ft, on the heading misalignment,  $\Delta\psi \pm 10$  deg, and with a total duration time not to exceed 45 sec. The maneuver is performed at an altitude of 10 ft ( $\pm 3$  ft), so that ground effects are not negligible and therefore were included in the vehicle model. Here again it is reasonable to consider the minimum time cost function expressed by Eq. (13).

The typical execution of the Pirouette maneuver can be divided into three phases. The first part is characterized by a transition from hover to a steady turn in lateral flight. The opposite transition is accomplished at the end of the maneuver when the hover state must be recovered. The central part of the maneuver is characterized by a steady turn with an appropriate angular velocity. The simulation strategy reflects this description, and it is effectively the result of two optimized maneuvers with a trim condition interposed between them.

The first and last transitions are formulated in exactly the same manner, except for the boundary conditions which are inverted; for the internal phase a steady turn in lateral flight at the velocity of 11 knots is assumed. Each transition is evaluated using a direct transcription approach using a Chebychev grid of 50 time elements and, according to the ADS-33 specification, the following additional constraints are enforced at each grid node:

$$|r(t_i) - R| \leq |\Delta R|, \quad |\psi(t_i) - \gamma(t_i)| \leq |\Delta\psi|, \quad (18)$$

$i = 0, \dots, N$ , where  $r(t) \triangleq \sqrt{x(t)^2 + y(t)^2}$  and  $\gamma(t) \triangleq \tan^{-1}(y(t)/x(t))$ , if  $x$ - $y$  is the plane of the reference circle centered in the origin.

For the first phase of the MTE, the final position and heading angle are not imposed directly, but additional constraints are used so that at the end of the maneuver the vehicle is located in an unknown point along the reference circle pointing its nose towards the center. The opposite approach is used for the last transition, where the initial position is unknown and constrained in an analogous way. Figure 11 shows the computed trajectory with snapshots of the vehicle. Figure 12 shows the roll and pitch angles, where one can notice the constant values corresponding to the central turning trim.

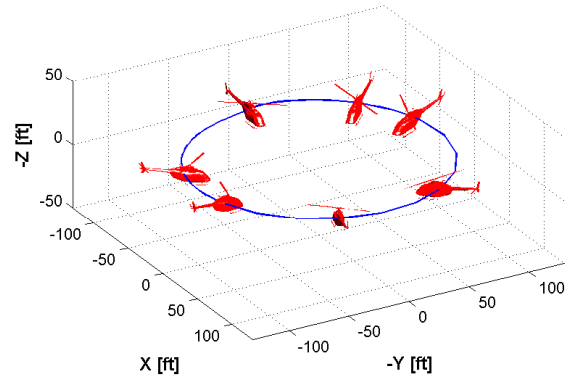


Figure 11: Pirouette MTE: view of the trajectory.

Next, we consider the Slalom MTE, shown in Fig. 13. The helicopter, starting from a stabilized forward flight condition lined up with the centerline of the test course, is supposed to turn around a series of obstacles and, finally to recover the initial steady state. The obstacles are located at 500 ft intervals and at  $\pm 50$  ft from the centerline; the obstacles should be passed with a maximum lateral error of 50 ft.

The maneuver must be accomplished below the reference altitude of 100 ft, so that, also in this case, ground effects must be included in the model. Furthermore, the maneuver definition does not assign a maximum time as in the previous case, but rather specifies

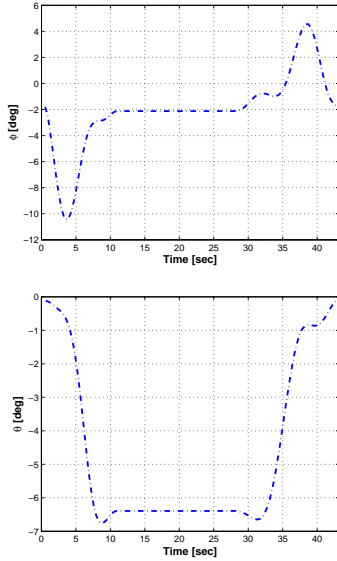


Figure 12: Pirouette MTE. Top: roll angle; bottom: pitch angle.

a minimum speed of at least 60 knots throughout the slalom.

The simulation is conducted using the direct transcription method, with a uniform grid of 100 steps and three obstacles. In order to introduce the presence of the obstacles, the bounds of Table 1 are enforced for the  $i$ th pylon, where  $x_j$  and  $y_j$  represent the position (in the  $x$ - $y$  plane) at the  $j$ th mesh node. A specific lower bound is imposed for the flight speed in order to guarantee the satisfaction of the lower value of 60 knots imposed by the ADS-33 specification. The minimum time cost function is used again to reach a proper level of aggressiveness. Figure 14 reports the optimal control time histories; the oscillations of the cyclics is related to the alternating left/right turns.

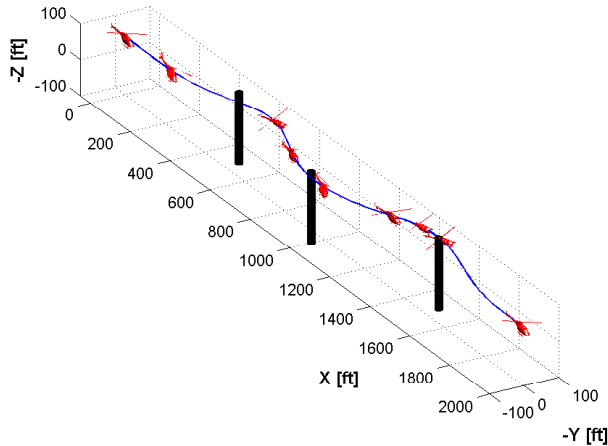


Figure 13: Slalom MTE: view of the trajectory.

	Lower	Upper
$x_{i25}$	$i$ 500 ft	$i$ 500 ft
$y_{i25}$	$-25 + (-1)^i$ 75 ft	$+25 + (-1)^i$ 75 ft

Table 1: Slalom. Position bounds for the obstacles.

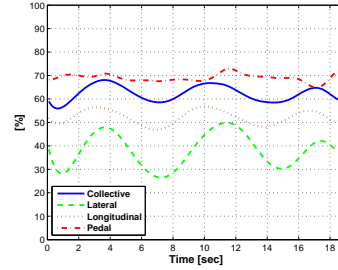


Figure 14: Slalom MTE: time history of control inputs.

### Engine-Off Landing

The last maneuver considered in this work represents a safe landing after a complete loss of engine power. The typical execution of such a maneuver can be subdivided into three phases:

- The first phase, characterized by loss of power, is a transition with variable engine RPM from an initial state to a stationary autorotative condition.
- The second phase is a steady state autorotation, which is maintained until an appropriate distance from the ground is reached.
- The final phase is a flare before touch-down. During this phase the pilot initially reduces the longitudinal cyclic pitch, controlling the horizontal velocity, augmenting the vehicle attitude and consequently the flow of air into the rotor disk and hence the rotor RPM. Immediately before ground impact, the pitch angle is reduced in order to avoid a tail strike, while the vertical velocity is controlled by a collective step command which subtracts energy from the rotor.

In the present analysis only the final flare maneuver is simulated, assuming that the helicopter is initially in a steady autorotation, with an initial horizontal speed of 40 knots; the vertical component (about -16 knots) is evaluated by using the zero torque condition. During the maneuver, the main rotor RPM must stay within the operational limits, where we assume a variation in the range  $\pm 10\%$  of the nominal value. At landing the pitch angle must be smaller than a maximum value dictated by the helicopter architecture (here the value of 12 deg is assumed), while the horizontal and vertical speeds are required to be smaller than limit values (40 knots and -4 knots, respectively) related to the landing gear structural limits.

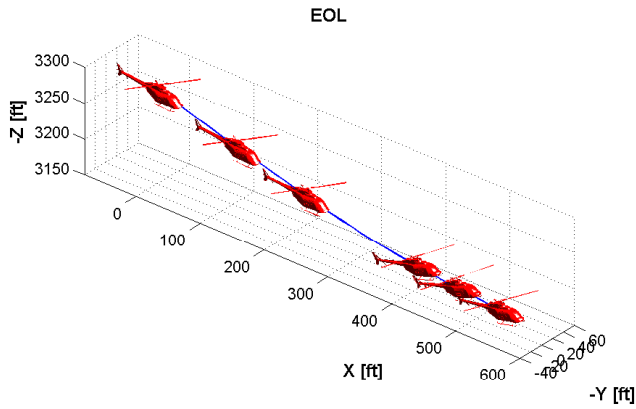


Figure 15: Engine-off landing: snapshots.

As in the case of the Category-A rejected take-off, a meaningful simulation policy for such a maneuver consists in the minimization of the altitude loss, according to Eq. (15).

The maneuver is evaluated by a multiple shooting approach, using a sufficient number of integration arcs so as to guarantee a good approximation in the required bounds for the RPM time history throughout the maneuver. The pitch angle time history, reported in Fig. 16, is characterized by a flare with a maximum value of about 20 deg, while the final value corresponds to the imposed critical limit of 12 deg. Figure 17 shows that the magnitude of the velocity components decrease during the maneuver, reaching values which are compatible with the landing gear capabilities. Figure 18 represents the collective time history, characterized by the typical step in the final seconds, which is strictly related to the reduction of the vertical velocity and the final decay of RPM from the upper to the lower bound shown in Fig. 19.

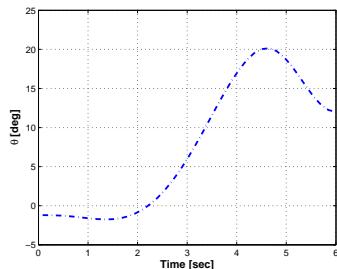


Figure 16: Engine-off landing: pitch angle.

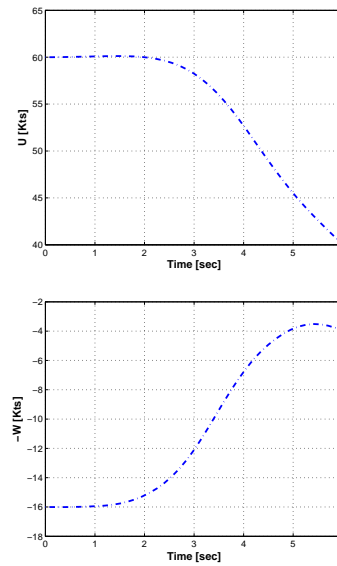


Figure 17: Engine-off landing: horizontal (top) and vertical (bottom) speeds.

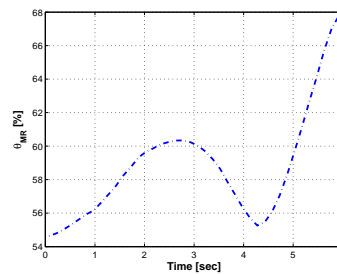


Figure 18: Engine-off landing: collective input.

## CONCLUDING REMARKS

In this work we have formulated a trajectory optimization approach to maneuver modeling in rotorcraft flight mechanics, including pilot-in-the-loop effects.

The formulation can accommodate the pilot control behavior as part of the definition of the cost function (and in this sense falls within the category of optimal control pilot models), as well as the command actuation and sensorial perception aspects. In this work, the command actuation was rendered using global equivalent models through the use of a simple delay in series with a second order filter. Although a more sophisticated model, as for example a biomechanical multi-body model, could be readily implemented in the formulation without conceptual difficulties, the present implementation is probably sufficient for capturing the relevant command actuation effects on the flight mechanics characteristics of the response. The sensorial perception component of the model was not considered here, mainly for the lack of sufficiently reliable data

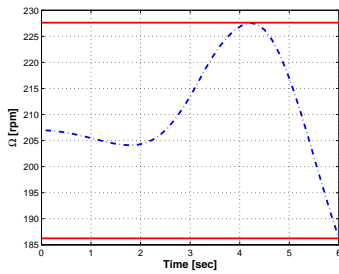


Figure 19: Engine-off landing: rotor angular speed.

for the tuning of the required Kalman-based observers; this aspect of the problem is currently under investigation, and will be reported in a forthcoming publication. It is reasonable to consider that the inclusion of the perception system model will determine further degradation of the performance, although the actual quantification of this aspect remains to be seen.

Based on the current state of this study, the following conclusions may be drawn:

- The performance degradation due to pilot-in-the-loop effects depends on the particular maneuver considered. In particular, it appears that for the Lateral Reposition MTE the pilot model induces negligible differences, while the Category-A rejected take-off shows a more pronounced effect with an increased altitude loss. Other maneuvers will be considered in the continuation of the present study. We have given here the pilot-off solutions for the Pirouette and Slalom MTEs, and an engine-off landing, which will be analyzed in the pilot-on case to try to quantify possible performance changes in these cases.
- The inclusion of a pilot model in the optimal control formulation does not imply substantial difficulties, since the coupled pilot-vehicle system is formally identical to a generic vehicle model expressed in non-linear state space form.
- The current version of the pilot model has only a modest impact on the computational cost of the optimization, so that the code retains its ability to conduct complete maneuver simulations in the order of minutes on standard desktop computers.
- As for all optimization problems, better performance and robustness of the procedures relies also on good initial guesses of the solution, which in this case also requires initial estimates of the internal pilot states. This was achieved here using a bootstrapping procedure, based on an initial solution computed without pilot model, followed by the initialization of the pilot states obtained with the computed pilot-off control inputs. This

procedure proved to be easy to implement and very effective.

## ACKNOWLEDGEMENTS

The present research is supported by AgustaWestland through a grant with the Politecnico di Milano, Marco Cicalé being the main project monitor. Simulations using the FLIGHTLAB code were conducted at the AgustaWestland headquarters in Cascina Costa, Italy, using AgustaWestland licenses. The contribution of C. Ravaioli and A. Ragazzi in the preparation of the examples is gratefully acknowledged.

## REFERENCES

- [1] *Advisory Circular 29-2C, Certification of Transport Category Rotorcraft*, Federal Aviation Administration, Department of Transportation, 1999.
- [2] *Handling Qualities Requirements for Military Rotorcraft*, Aeronautical Design Standard, U.S. Army Aviation and Missile Command, Aviation Engineering Directorate, Rept. ADS-33E-PRF, Redstone Arsenal, AL, 2000.
- [3] Advanced Rotorcraft Technology, Inc., 1685 Plymouth Street, Suite 250, Mountain View, CA 94043, <http://www.flightlab.com>.
- [4] Ascher, U.M., Mattheij, R.M.M., and Russell, R.D., *Numerical Solution of Boundary Value Problems for Ordinary Differential Equations*, Classics in Applied Mathematics, 13, SIAM, Philadelphia, 1995.
- [5] Betts, J.T., *Practical Methods for Optimal Control using Non-Linear Programming*, SIAM, Philadelphia, 2001.
- [6] Betts, J.T., "Survey of Numerical Methods for Trajectory Optimization," *Journal of Guidance, Controls and Dynamics*, Vol. 21(2), 1998, pp. 193–207.
- [7] Bottasso, C.L., and Croce, A., "Optimal Control of Multibody Systems using an Energy Preserving Direct Transcription Method," *Multibody Systems Dynamics*, Vol. 12, 2004, pp. 17–45.
- [8] Bottasso, C.L., Croce, A., Leonello, D., and Riviello, L., "Optimization of Critical Trajectories for Rotorcraft Vehicles," *Journal of the American Helicopter Society*, Vol. 50, 2005, pp. 165–177.
- [9] Bottasso, C.L., Croce, A., Leonello, D., and Riviello, L., "Rotorcraft Trajectory Optimization with Realizability Considerations," *Journal of Aerospace Engineering*, Vol. 18, 2005, pp. 146–155.

- [10] Bottasso, C.L., Chang, C.-S., Croce, A., Leonello, D., and Riviello, L., "Adaptive Planning and Tracking of Trajectories for the Simulation of Maneuvers with Multibody Models," *Computer Methods in Applied Mechanics and Engineering*, Special Issue on Computational Multibody Dynamics, Vol. 195, 2006, pp. 7052–7072.
- [11] Bottasso, C.L., Maisano, G., and Scorcelletti, F., "Trajectory Optimization Procedures for Rotorcraft Vehicles, their Software Implementation and Applicability to Models of Varying Complexity," American Helicopter Society 64th Annual Forum, Montréal, Canada, April 29–May 1, 2008; also: *Journal of the American Helicopter Society*, under review, 2008.
- [12] Bottasso, C.L., Scorcelletti, F., Maisano, G., Cicalè, M., and Ragazzi, A., "Mission Task Elements and Critical Maneuvers Simulation for Rotorcraft Vehicles," Rotorcraft Handling Qualities Conference, University of Liverpool, Liverpool, UK, November 4–6, 2008.
- [13] Bottasso, C.L., "Solution Procedures for Maneuvering Multibody Dynamics Problems for Vehicle Models of Varying Complexity," *Multibody Dynamics — Computational Methods and Applications*, C.L. Bottasso, Ed., Computational Methods in Applied Sciences, ISBN 978-1-4020-8828-5, Springer-Verlag, Dordrecht, The Netherlands, 2008.
- [14] Bradley, R., MacDonald, C.A., and Buggy, T.W., "Quantification and Prediction of Pilot Workload in the Helicopter/Ship Dynamic Interface," *Journal of Aerospace Engineering*, Vol. 219(5), 2005, pp. 429–443.
- [15] Bryson, A.E., and Ho, Y.C., *Applied Optimal Control*, Wiley, New York, 1975.
- [16] Davidson, J.B., and Schmidt, D.K., "Modified Optimal Control Pilot Model for Computer-Aided Design and Analysis," NASA, Technical Memorandum 4348, 1992.
- [17] Frazzoli, E., "Robust Hybrid Control for Autonomous Vehicle Motion Planning," Ph.D. Thesis, Department of Aeronautics and Astronautics, Massachusetts Institute of Technology, Cambridge, MA, USA, 2001.
- [18] Gill, P.E., Murray, W., and Wright, M.H., *Practical Optimization*, Academic Press, London and New York, 1981.
- [19] Hess, R.A., "Unified Theory for Aircraft Handling Qualities," *Journal of Guidance, Control and Dynamics*, Vol. 20(6), 1997, pp. 1141–1148.
- [20] Hess, R.A., "Simplified Technique for Modelling Piloted Rotorcraft Operations Near Ships," *Journal of Guidance, Control and Dynamics*, Vol. 29(6), 2006, pp. 1339–1349.
- [21] Höene, G., "Computer Aided Development of Biomechanical Pilot Models," *Aerosp. Sci. Technol.*, Vol. 4, 2000, pp. 57–69.
- [22] Jagacinski, R.J., *Control Theory for Humans — Quantitative Approaches to Modeling Performance*, Erlbaum, Mahwah, NJ, 2003.
- [23] Kleinman, D.L., Baron, S., and Levison, W.H., "An Optimal Control Model of Human Response. Part I: Theory and Validation. Part II: Prediction of Human Performance in a Complex Task," *Automatica*, Vol. 6, 1970, pp. 357–383.
- [24] Kramer, U., "On the Application of Fuzzy Sets to the Analysis of the System-Driver-Vehicle Environment," *Automatica*, Vol. 3(1), 1985, pp. 101–107.
- [25] McRuer, D.T., and Krendel, E., "Mathematical Models of Human Pilot Behavior," AGARD-AG-188, 1974.
- [26] Prouty, R.W., *Helicopter Performance, Stability, and Control*, R.E. Krieger Publishing Co., Malabar, 1990.
- [27] Van Paassen, R., "Biophysics in Aircraft Control: A Model of the Neuromuscular System of the Pilot's Arm," Ph.D. Dissertation, Faculty of Aerospace Engineering, Delft University of Technology, The Netherlands, 1994.
- [28] Veeraklaew, T., and Agrawal, S.K., "New Computational Framework for Trajectory Optimization of Higher-Order Dynamic Systems," *Journal of Guidance, Control and Dynamics*, Vol. 24(2), 2001, pp. 228–236.
- [29] Zeyada, Y., and Hess, R.A., "Modelling Human Pilot Cue Utilization with Application to Simulator Fidelity Assessment," *Journal of Aircraft*, Vol. 37(4), 2000, pp. 558–597.